



Study on signal characteristics of burst tendency coal under different loading rates

Chao Zhou^{1,2} · Xueqiu He^{1,2} · Dazhao Song^{1,2} · Zhenlei Li^{1,2} · Huakang Yang^{1,2} · Yang Liu^{1,2} · Lei Guo^{1,2}

Received: 19 March 2022 / Revised: 12 May 2022 / Accepted: 15 July 2024
© The Author(s) 2024

Abstract

In order to study the mechanics, acoustic emission (AE) and electromagnetic emission (EME) response law of bursting liability coal at different loading rates, uniaxial compression tests were carried out on coal mass from Konggu Coal Mine. The corresponding relations among mechanical properties, AE and EME signals in the process of coal failure under loading were analyzed, and the energy evolution law of coal failure with bursting liability under loading rate was discussed. The results show that within a certain range of loading rate, the higher the loading rate, the higher the compressive strength and peak load of bursting liability coal, and the shorter the time for coal to reach the peak load. Under different loading rates, the mechanics, AE and EME signals of coal samples can be well corresponded. When the loading rate is low, the number of blocks destroyed of coal sample is large and the block size is relatively small, and the blocks are mainly scattered around the test platform. When the loading rate is high, the number of damaged blocks is relatively small and the block size is relatively large, and the blocks are far away from the test bench. When loading at a low rate, the internal cracks in coal can be fully developed and connected, and the energy release rate is relatively uniform in the process of loading and failure of coal sample. In the case of high loading rate, the energy release rate of coal sample in the loading process is much smaller than that in the moment of failure. Combining the above test results with the actual situation of the working face, it can be concluded that the total energy stored in the coal of fast mining increases and the threshold of impact decreases compared with that of slow mining. Therefore, under the disturbance of external dynamic load, rapid mining is more likely to induce rock burst.

Keywords Loading rate · Burst tendency · The mechanics · AE and EME response · Block damage · Energy release rate · Mining speed · Rock burst

1 Introduction

The increase in the mining speed of the working face will lead to a larger roof subsidence per unit time, the effect of which is equivalent to the increase in the loading rate of the roof rock on the coal seam (Chen et al. 2009; Feng et al. 2019; Liang et al. 2016). The change in the loading rate will have an impact on the mechanical properties of the coal seam, and also on the AE and EME signal released by the

loading process of the coal seam (Mahmutoğlu 2005; Xue et al. 2016; He et al. 2022; Zhang et al. 2017).

At present, experts and scholars have carried out extensive research on the properties of coal seam under different loading rates, and have obtained abundant results (Wang et al. 2009; Yin et al. 2010; Huang and Liu 2013; Sang et al. 2013; Hudson et al. 1971).

On a laboratory scale, Pan et al. (2013) explored the charge induction law under uniaxial compression at different loading rates, and concluded that the maximum value of charge induction in coal mass occurs before the stress reaches its ultimate strength. Xiao et al. (2017) investigated the effect of loading rate on the acoustic-charge of coal rupture process, and concluded that the change of acoustic-charge signal generated by the coal rock rupture process under different loading rates is in good agreement with the stress mutation of the loaded coal rock. Li et al. (2015) studied the influence of loading rate on the

✉ Xueqiu He
hexq@ustb.edu.cn

¹ School of Civil and Resources Engineering, University of Science and Technology Beijing, Beijing 100083, China

² Key Laboratory of Ministry of Education for Efficient Mining and Safety of Metal Mine, University of Science and Technology Beijing, Beijing 100083, China

mechanical behavior of coal samples, and concluded that the strength of coal increased first and then decreased with the increase of loading rate. When the loading rate is lower than the critical loading rate, the coal sample strength increases with the increase of the loading rate. when the loading rate is higher than the critical loading rate, the strength decreases with the increase of the loading rate. Jiang et al. (2014) studied the influence of loading rate on energy accumulation and dissipation, and believed that the increase of loading rate would cause energy dissipation and accumulation to occur earlier, and the maximum elastic energy storage density had a positive exponential relationship with loading rate.

In terms of engineering site, Zhao et al. (2018) studied the energy accumulation and release of coal seam roof under the influence of working face mining speed, and believed that with the increase of loading rate, the accumulated energy of rock beam showed an exponential increase trend, and so did the energy release of roof. Liu et al. (2018) studied the effect of coal mine rock burst mining speed, and concluded that high speed and uneven speed mining were easy to induce rock burst through field cases. Xie et al. (2007) studied the influence of mining speed on mechanical characteristics of surrounding rock in fully mechanized caving face. It is concluded that the failure zone and displacement of coal and rock mass decrease with the increase of advancing velocity of working face, and the front abutment pressure peak position is close to the coal wall of working face. Wang et al. (2006) studied the influence of mining rate on surrounding rock stress environment, and concluded that with the increase of working face speed, the peak stress in front of the working face approached the working face, the deformation time of surrounding rock mass shortened, and the displacement of surrounding rock mass decreased.

The above scholars have either studied the charge induction pattern and mechanical behaviour of coal samples under different loading rates from a laboratory perspective, or explored the effect of recovery rate on the rock burst from an engineering site. But few have used the means of both together for the study of burst-tendency coal samples and to guide the prevention and control of rock burst.

To this end, this paper used laboratory experiments, theoretical analysis and field measurement to explore the acoustic, electrical and mechanical characteristics of bursting liability coal samples under different loading rates, and explained the mechanism of the characteristics in the test. At the same time, based on the experimental results, this paper expounds the influence of different mining speed on rock burst, in order to provide experimental basis and theoretical basis for determining reasonable mining speed of rock burst.

2 Experimental design and methods

2.1 Sample preparation

The coal samples used in this experiment were taken from the raw coal at Konggou Coal Mine, which was identified by the appraisal agency as an burst tendency coal seam. The samples were processed according to the standards of the International Society of Rock Mechanics, and were made into cylinders of $\Phi 50 \times 100$ mm by core drilling, cutting and grinding. Some coal samples with fissures were removed and those with good surfaces were selected for testing, and the formed samples are shown in Fig. 1. Three groups of representative coal samples were selected and named as Sample 1 to Sample 3. The basic physical parameters of each sample are shown in Table 1.

2.2 Experimental system

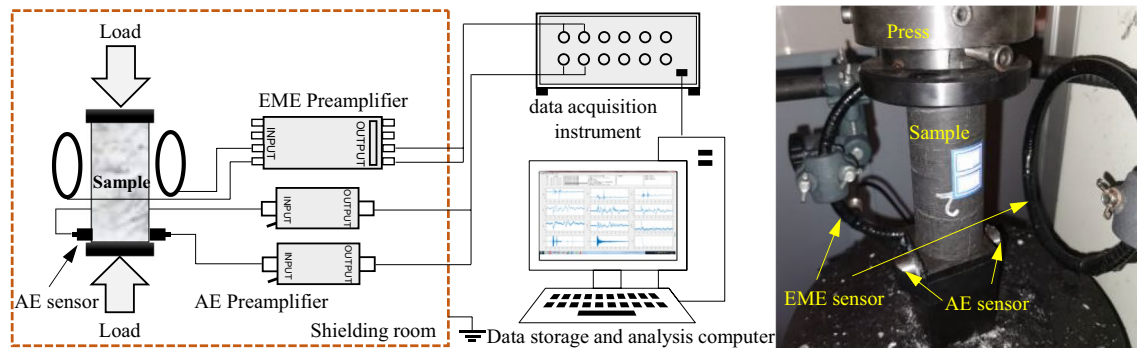
The loading system for this experiment uses the YAW-600 microcomputer-controlled electro-hydraulic servo pressure tester, which has a load resolution of 3 N and a displacement resolution of 0.3 μm . The acoustic and electrical data acquisition system uses a home-made high-speed data acquisition system, which has 12 channels, a maximum acquisition frequency of 10 MHz, an input signal voltage range of ± 5 V and an input impedance of 50 Ω . The response frequency range of the acoustic emission sensor is 50–400 kHz, and the bandwidth is 20–1500 kHz. The electromagnetic radiation sensor uses a ring magnetic field antenna SAS-560, with a frequency range of 20 Hz–2 MHz, the antenna plane is parallel to the loading direction and placed at a position facing the sample of 6.5 cm; the amplification of the electromagnetic radiation power amplifier is 80 dB, and the frequency range is 10 kHz–10 MHz. The experiment was carried out in an electromagnetic shielded room to reduce the interference of the external electromagnetic field on the experimental signal, and the experimental system is shown in Fig. 2.



Fig. 1 Physical drawing of the sample

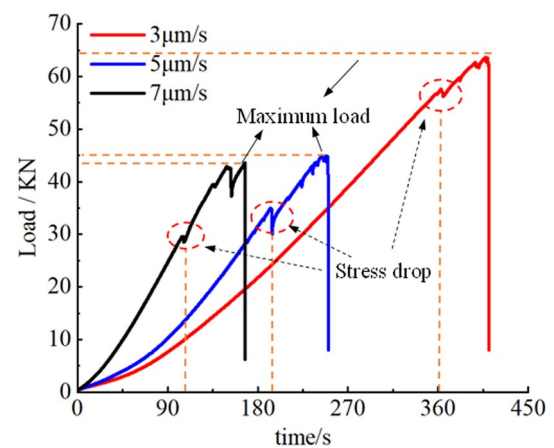
Table 1 Physical parameters of sample

Sample No.	Height (mm)	Diameter (mm)	Quality (g)	Density (g/cm ³)
Sample 1	100.20	49.42	256.51	1.335
Sample 2	100.38	49.30	256.87	1.341
Sample 3	100.34	49.32	255.24	1.332
Average	100.17	49.39	256.19	1.335

**Fig. 2** Diagrammatic drawing of the experimental system

2.3 Experimental scheme

In this experiment, displacement-controlled uniaxial compression loading was applied to three groups of coal samples, and the loading rates were divided into 3 $\mu\text{m/s}$, 5 $\mu\text{m/s}$ and 7 $\mu\text{m/s}$. The loading rates were kept constant until the samples were damaged. Using the built acousto-electric synchronous test system, the AE and EME signals during the uniaxial compression damage of the sample are collected and stored synchronously throughout the process, and the response characteristics are statistically analysed in terms of ringing counts and energy. The sampling frequency of the press is 50 Hz and the sampling frequency of the AE and EME signal collector is 2 MHz.

**Fig. 3** Load-time curves for burst-prone coal samples at different loading rates

3 Experimental results and analysis

3.1 Mechanical properties of coal at different loading rates

Figure 3 shows the mechanical properties of burst prone coal samples at different loading rates. From the load-time curves of the coal samples, the loading damage can be divided into four stages throughout, i.e. compression-density stage, elastic stage, accelerated damage stage and complete damage stage.

At low speed loading (3 $\mu\text{m/s}$), the time for the first stress drop to occur is about 360 s and the time to reach peak damage is about 410 s. The peak stress for burst prone coal samples is about 63.5 MPa, and the time for

the first stress drop to occur is about 85% of the total time for loading damage. At medium speed loading (5 $\mu\text{m/s}$), the time for the first stress drop to occur is approximately 185 s, the time to reach peak stress is approximately 243 s, and the peak stress in the coal sample is approximately 45 MPa. The time for the first stress drop to occur is approximately 76% of the total time of loading damage, and the time from the first stress drop to the final damage is approximately 24% of the total time. At high speed loading (7 $\mu\text{m/s}$), the time for the first stress drop to occur is approximately 100 s, the time to reach peak stress is approximately 166 s, and the peak stress in the coal sample is approximately 43 MPa. The time for the first stress

drop to occur is approximately 60% of the total time for loading damage, and the time from the first stress drop to the final damage is approximately 40% of the total time for loading damage.

According to Fig. 3 and Table 2, with the increase of loading rate, the peak load of bursting liability coal decreases, the time for coal to reach peak stress shortenes, and the compressive strength of coal decreases. The maximum rate of change in both peak load and compressive strength exceeds 45%, the time for the first stress drop to occur is advanced, and the time from the first stress drop to the final destruction of the coal as a percentage of the total loading time increases.

This is due to the fact that as the loading rate increases, the time for the original fracture to close is shortened, the time for new cracks to appear is advanced, and the time for the stress drop to appear is also advanced. The compression and elastic phases of the samples with burst prone account for a high proportion of the whole damage process, and the coal reaches the peak stress and then falls rapidly, there is no post-peak residual stress. After loading failure, the integrity of the residual main body of the sample is poor, and the bearing capacity of the coal is more similar to that of the rock mass, and the coal is finally brittle failure.

It can be seen that the increase of loading rate has a great influence on the mechanical properties of coal. Under slow loading, the cracks inside the bursting liability coal sample can be fully closed and developed, and the coal mass shows high compressive strength. The time of stress drop is relatively later, and the energy is fully dissipated as well as fully accumulated.

When the loading rate increases, the original cracks in the coal mass will close in a short time, while the new cracks are not fully developed, the compressive strength of the coal mass will decrease relatively, and the time of stress drop will appear in advance. The higher the loading rate the lower the peak load on the coal seam, the lower the compressive strength, the shorter the time to destruction, the smaller the load threshold that needs to be destroyed, and the easier it is for the coal seam to be burst damaged by external disturbances.

Table 2 Mechanical properties test results for burst-prone coal samples

No.	Peak loads (kN)	Compressive strength (MPa)	Elastic modulus (GPa)
1	63.66	33.20	2.556
2	44.96	23.56	1.567
3	43.64	22.85	1.982

3.2 Experimental results of acoustic and electrical response of coal samples

Figures 4, 5 and 6 shows the AE and EME responses of coal samples with bursting liability during uniaxial compression. In the experiment, the threshold value of EME signal is set as 0.02 V, and that of AE signal was set as 0.2 V. Two parameters of acoustic signal are ringing count and energy.

As can be seen from Figs. 4, 5 and 6, AE and EME signals of coal samples in the first half of low, medium and high loading rates are relatively small. At low speed, only sporadic AE signals appear at the initial stage of coal sample loading, while EME signals are almost absent. At medium speed, AE and EME radiation signal do not appear. When loading at high speed, AE signals appear in about 50 s, and EME signals appear in about 100 s. With the loading process, the first stress drop occurs at 360 s, 180 s and 120 s at

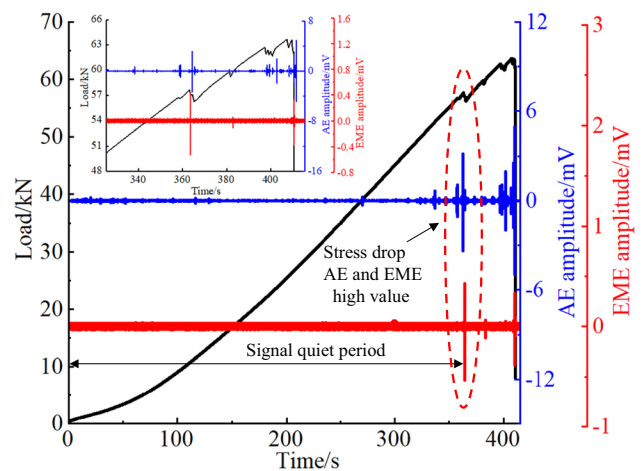


Fig. 4 Correspondence between load-AE /EME amplitude at 3 μm/s loading rate

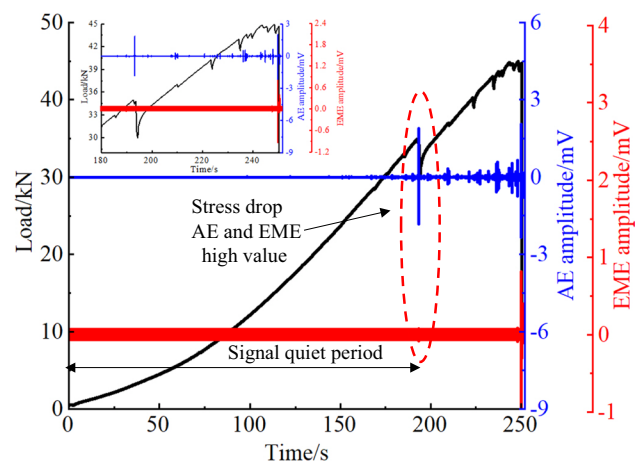


Fig. 5 Correspondence between load-AE /EME amplitude at 5 μm/s loading rate

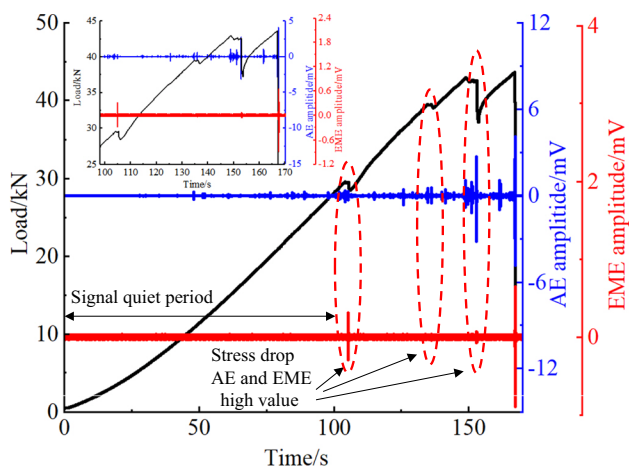


Fig. 6 Correspondence between load-AE /EME amplitude at 7 μm/s loading rate

low, medium and high loading rates, accompanied by the appearance of first high value in the AE and EME signal. The faster the loading rate, the earlier the first stress drop. After the first stress drop, AE and EME signals begin to be abundant. When the sample is loaded at low speed to 400 s, medium speed to 250 s, and high speed to 180 s, the loading stress reaches peak value, AE and EME signal also reaches peak value, and the main fracture failure occurs. AE signal and EME signal were not received after the destruction of the sample, and the sample was completely destroyed at one time. In the loading process, the time of EME signal is generally later than that of AE signal, and the high value of AE signal is generally greater than that of EME signal.

Table 3 and shows Table 4 the statistical results of ringing count and energy of samples. It can be seen from the table that the maximum value and cumulative value of AE ringing count increase with the increase of loading rate, while the maximum value and cumulative value of acoustic emission

energy change little with the increase of loading rate. The maximum value of EME count and energy accounts for more than 75% of the respective cumulative value, and the maximum and cumulative value are close to each other. The maximum and cumulative value do not change regularly with the change of loading rate. The EME signal mainly appears in the final peak destruction stage.

Ringing count reflects the fluctuation of signal per unit time, and the larger the count is, the more frequent the signal fluctuation is. In the experiment, with the increase of loading rate, the maximum count value and cumulative value also increase. This indicates that with the increase of loading rate, more cracks in the sample are fully connected, developed and destroyed in a short time, releasing a large amount of energy.

3.3 Degree of breakage of coal samples under different loading rates

Failure modes of coal samples at different loading rates are shown in Fig. 7. The quantity and quality statistics of coal with different lumpiness after coal sample destruction are shown in Tables 5 and 6, The statistical method of damaged coal samples is shown in Fig. 8.

It can be seen from Tables 4 and 5 that in the range of 0–5 mm, with the increase of loading rate, the quality and quantity of coal with small lumpiness begin to decrease. In the range of 50–100 mm, the bulk coal quality and quantity decrease with the increase of loading rate. In the range of 5–50 mm, the loading rate is mainly medium and low.

According to Fig. 8, Tables 5, 6, and field experimental observation, when the loading rate is low, the number of blocks after coal sample failure is large and the lumpiness is relatively small. Blocks are mainly scattered around the test platform, and the sound at the moment of coal sample failure is relatively small. When the loading rate is high,

Table 3 Statistics of ringing counts results of samples

No.	Maximum AE count	AE Cumulative value count	Proportion (%)	EME count maximum	EME Count cumulative value	Proportion (%)
1	1423	4579	31	280	350	80
2	2333	4235	55	408	466	87
3	3973	9120	43	268	339	79

Table 4 Statistical table of sample energy results

No.	Maximum AE energy	Cumulative AE energy value	Proportion (%)	EME maximum energy	EME energy accumulative value	Proportion (%)
1	7679	12,700	60	1466	1956	75
2	5224	7118	73	3701	3800	97
3	7635	13,327	57	2393	2805	85

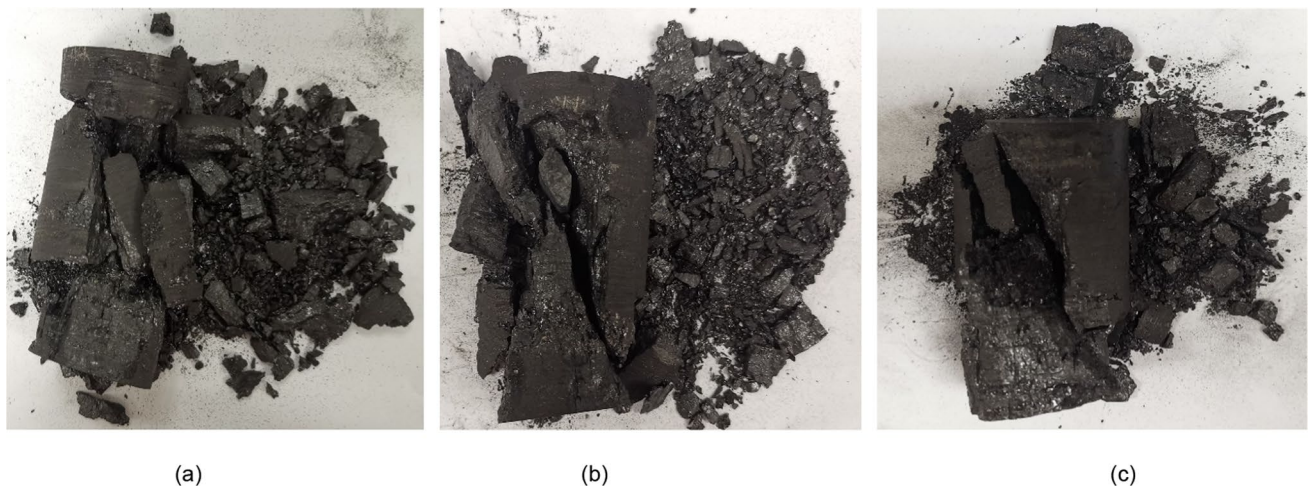


Fig. 7 Failure modes of coal samples under different loading rates. **a–c** Represent the failure modes of coal samples under low, medium and high loading rates respectively

Table 5 Quantity statistics of different lumpiness of coal samples after destruction

No.	2.5–5.0 (mm)	5.0–10 (mm)	10–15 (mm)	15–20 (mm)	20–30 (mm)	30–40 (mm)	40–50 (mm)	50–100 (mm)	Max (mm)
1	143	13	8	3	3	3	2	1	55.3
2	120	56	13	8	8	2	5	2	83.9
3	110	45	2	9	3	0	1	3	75.1

Table 6 Quality statistics of different lumpiness of coal samples after destruction

No.	0–5.0 (mm)	5.0–10 (mm)	10–15 (mm)	15–20 (mm)	20–30 (mm)	30–40 (mm)	40–50 (mm)	50–100 (mm)	Max
1	24.37	3.73	2.81	1.38	8.28	16.40	108.14	43.87	43.87
2	12.81	5.42	3.63	4.16	7.20	10.81	102.87	87.73	71.18
3	10.97	6.10	0.54	7.78	6.12	0	9.81	157.85	83.49



Fig. 8 Statistics of coal samples with different lumpiness after coal sample destruction

the number of blocks destroyed by coal sample is relatively small and the lumpiness is relatively large. Blocks are far away from the test platform, and a "bang" can be heard at the moment of failure.

Combined with the phenomena and results of experimental statistics, it can be seen that with the increase of loading rate, the number of blocks decreases after coal sample damage, but the lumpiness increases. The reason is that under low rate loading, the internal cracks in coal seam can be fully developed and connected, and the energy release rate is relatively uniform in the process of loading and failure of coal sample, and the failure of coal sample is more thorough. Under high rate loading, the coal sample has rapid energy and release energy in a short time, and the failure form of coal sample appears in the shape of large blocks. The energy release rate in the loading process of coal sample is far less than that in the moment of its destruction.

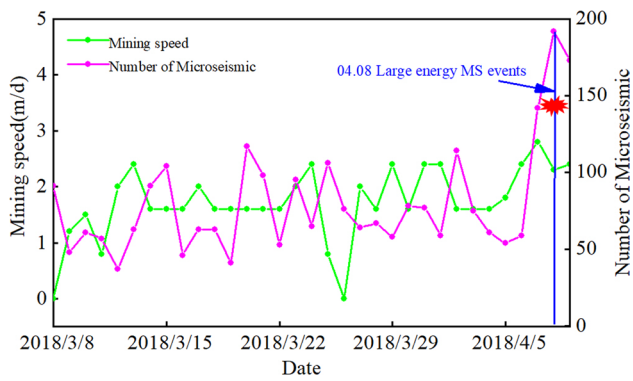


Fig. 9 Relationship between mining speed and microseismic frequency before high-energy MS event on 8 April

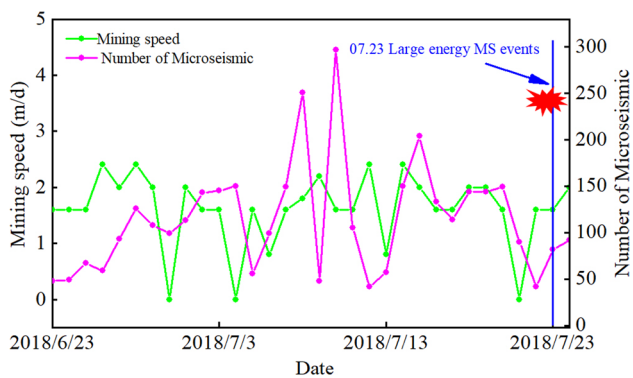


Fig. 10 Relationship between mining speed and microseismic frequency before high-energy MS event on July 23

4 Field practice

In order to establish the relationship between laboratory tests and working face site, the relationship between mining speed and microseismic (MS) event frequency of working face in Konggou Coal mine is analyzed.

4.1 Relationship between mining speed and microseismic event frequency

The corresponding relationship between mining speed and MS event frequency of one month before the occurrence of "April 8" and "July 23" high-energy MS event is shown in Figs. 9 and 10.

It can be seen from Figs. 9 and 10 that there is a good correspondence between the mining speed and the frequency of MS events. When the mining speed increases, the frequency of MS events is in a high range. When the mining speed decreases, the frequency of MS events is in

a low range. When the mining speed is in the period of rising or continuous high speed fluctuation, the frequency of MS events is in an abnormally active period, but the variation of MS frequency lags behind that of mining speed.

It can be seen from Figs. 9 and 10 that there is a good correspondence between the mining speed and the frequency of MS events. When the mining speed increases, the frequency of MS events is in a high range. When the mining speed decreases, the frequency of MS events is in a low range. When the mining speed is in the period of rising or continuous high speed fluctuation, the frequency of MS events is in an abnormally active period, but the variation of MS frequency lags behind that of mining speed.

Before the occurrence of "April 8" and "July 23" large energy MS events, the mining speed was either in a continuous high-speed mining, or in a rapid uptrend.

4.2 Principle that mining speed affects the frequency of MS events

Suppose the working face is mined at two speeds V_1 and V_2 , where V_1 represents slow mining and V_2 represents fast mining, and V_2 is greater than V_1 . The distances of L_1 and L_2 are retrieved in the same number of days t . L_1 and L_2 are calculated as shown in Eqs. (1) and (2), so that L_2 is greater than L_1 , as shown in Fig. 11.

$$L_1 = V_1 t \tag{1}$$

$$L_2 = V_2 t \tag{2}$$

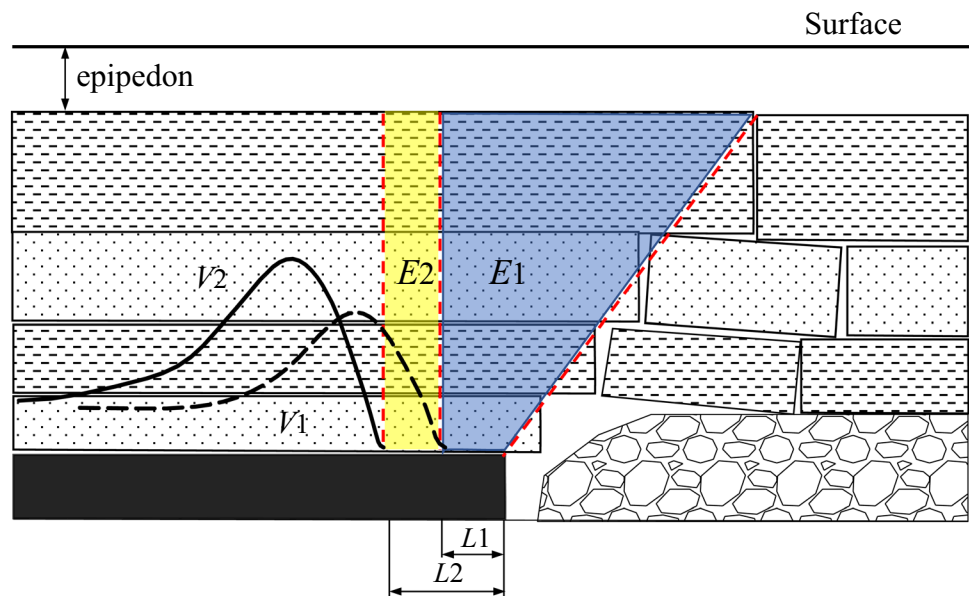
where L_1 and L_2 are in m, V_1 and V_2 are in m/d, and t is in d.

When the upper strata does not reach the fracture step, the range of strata affecting the working face stress during slow V_1 mining is E_1 , and the corresponding leading stress is σ_1 curve. During fast V_2 mining, the range of rock strata affecting the working face stress is $E_1 + E_2$, and the corresponding advance stress is σ_2 curve. The larger the range of rock strata affecting the stress at the working face, the larger the peak value and wider the range of its corresponding advance bearing stress. Therefore, the peak value and influence range of σ_2 curve are much larger than that of σ_1 curve, as shown in Fig. 11.

As can be seen from Fig. 11, rapid mining of working face causes the coal seam to be affected by a wider range of rock strata, and the peak value and range of advance stress will increase compared with slow mining, so the rapid mining face faces greater rock burst.

According to the results of laboratory tests and field observations, more energy is accumulated and less energy is dissipated in rapid mining than in slow mining, and the load threshold of coal body destruction is smaller. Therefore, the total energy stored in coal increases and the impact threshold

Fig. 11 Mechanism diagram of mining speed affecting rock burst. In the figure, L_1 represents the distance of low-speed mining and L_2 represents the distance of high-speed mining. σ_1 represents the advance stress at low speed mining, and σ_2 represents the advance stress at high speed mining. E_1 is the range of rock strata affecting the working face stress during low-speed mining, and E_2 represents the range of increased rock strata affecting the working face stress during high-speed mining



decreases. Under the disturbance of external dynamic load, rapid mining is more likely to induce rock burst.

5 Conclusions

- (1) The change of loading rate will affect the mechanical properties of bursting liability coal samples. Within a certain range of loading rate, the higher the loading rate, the higher the compressive strength and peak load of bursting liability coal, and the shorter the time for coal to reach the peak load.
- (2) Under different loading rates, the mechanics, AE and EME signals of coal samples can be well corresponded. When there is a stress drop, the AE and EME signals have relatively high values. When the stress reaches the peak, the two signals also reach the maximum value. The maximum value and cumulative value of AE count increase with the acceleration of loading rate. On average, the AE signal value of fast loading is greater than that of slow loading.
- (3) When the loading rate is low, the number of blocks destroyed of coal sample is large and the block size is relatively small, and the blocks are mainly scattered around the test platform. When the loading rate is high, the number of damaged blocks is relatively small and the block size is relatively large, and the blocks are far away from the test bench.
- (4) When loading at a low rate, the internal cracks in coal body can be fully developed and connected, and the energy release rate is relatively uniform in the process of loading and failure of coal sample. In the case of high loading rate, the energy release rate of coal sample

in the loading process is much smaller than that in the moment of failure.

- (5) In the field production, the peak value and range of coal advance stress are increased by rapid mining. Compared with slow mining, rapid mining accumulates more energy in a short period of time, but dissipates less energy, and the total energy stored in coal increases. At the same time, the threshold value of coal impact is relatively lower in rapid mining. Therefore, under the disturbance of dynamic load, rapid mining is more likely to induce rock burst than slow mining.

Funding Supported by the National Natural Science Foundation of China (52304203, 52374180 and 52327804).

Declarations

Conflict of interest The authors have no conflict of interest for the publication of this paper.

Open Access This article is licensed under a Creative Commons Attribution 4.0 International License, which permits use, sharing, adaptation, distribution and reproduction in any medium or format, as long as you give appropriate credit to the original author(s) and the source, provide a link to the Creative Commons licence, and indicate if changes were made. The images or other third party material in this article are included in the article's Creative Commons licence, unless indicated otherwise in a credit line to the material. If material is not included in the article's Creative Commons licence and your intended use is not permitted by statutory regulation or exceeds the permitted use, you will need to obtain permission directly from the copyright holder. To view a copy of this licence, visit <http://creativecommons.org/licenses/by/4.0/>.

References

- Chen M, Zhang Y, Jin Y (2009) Experimental study of influence of loading rate on Kaiser effect of different lithological rocks. *Chin J Rock Mech Eng* 28(5):2599–2604
- Feng LF, Dou LM, Wang XD (2019) Mechanism of mining advance speed on energy release from hard roof movement. *J China Coal Soc* 44(11):3329–3339
- He S, Mengli Q, Liming Q, Dazhao S, Xiufeng Z (2022) Early warning of coal dynamic disaster by precursor of AE and EMR “quiet period.” *Int J Coal Sci Technol* 9(1):46. <https://doi.org/10.1007/s40789-022-00514-z>
- Huang BX, Liu JW (2013) The effect of loading rate on the behavior of samples composed of coal and rock. *Int J Rock Mech Min Sci* 61:23–30
- Hudson JA, Brown ET, Fairhurst C (1971) Optimizing the control of rock failure in servo-controlled laboratory tests. *Rock Mech* 3(4):217–224
- Jiang YD, Li HT, Zhao YX (2014) Effect of loading rate on energy accumulation and dissipation in rocks. *J China Univ Min Technol* 43(03):369–373
- Li HT, Jiang CX, Jiang YD (2015) Mechanical behavior and mechanism analysis of coal samples based on loading rate effect. *J China Univ Min Technol* 44(03):430–436
- Liang CY, Li X, Wu SR (2016) Research on energy characteristics of size effect of granite under low/intermediate strain rates. *Rock Soil Mech* 37(12):3472–3480
- Liu JH, Sun H, Tian ZJ (2018) Effect of advance speed on rock burst in coal mines and its dynamic control method. *J China Coal Soc* 43(7):1858–1865
- Mahmutoğlu Y (2005) The effects of strain rate and saturation on a micro-cracked marble. *Eng Geol* 82(3):137–144
- Pan YS, Tang Z, Li ZH, Li GZ (2013) Research on the charge inducing regularity of coal rock at different loading rate in uniaxial compression tests. *Chin J Geophys* 56(3):1043–1048
- Sang HC, Yuji O, Katsuhiko K (2013) Strain-rate dependency of the dynamic tensile strength of rock. *Int J Rock Mech Min Sci* 40(5):763–777
- Wang JA, Jiao SH, Xie GX (2006) Study on influence of mining rate on stress environment in surrounding rock of mechanized top caving mining face. *Chin J Rock Mech Eng* 25(5):1–7
- Wang EY, He XQ, Li ZH (2009) EMR technology of coal or rock and its application. Science Press, Beijing
- Xiao XC, Ding X, Zhao X (2017) Experimental study on acoustic emission and charge signals during coal failure process at different loading rates. *Rock Soil Mech* 38(12):3419–3426
- Xie GX, Chang JC, Hua XZ (2007) Influence of mining velocity on mechanical characteristics of surrounding rock in fully mechanized top-coal caving face. *Chin J Geotech Eng* 07:963–967
- Xue DL, Zhou HW, Wang ZH (2016) Failure mechanism and mining-induced mechanical properties of coal under different loading rates. *J China Coal Soc* 41(3):595–602
- Yin XT, Ge XR, Li CG, Wang SL (2010) Influences of loading rates on mechanical behaviors of rock materials. *Chin J Rock Mech Eng* 29(S1):2610–2615
- Zhang HW, Li YP, Chen Y (2017) Study on safety pushing forward speed of island coal mining face under hard roof and hard seam and hard floor conditions. *Coal Sci Technol* 45(02):6–11
- Zhao TB, Guo WY, Han F (2018) Analysis on energy accumulation and release of roof under influence of mining speed. *Coal Science and Technology* 46(10):37–44

Publisher's Note Springer Nature remains neutral with regard to jurisdictional claims in published maps and institutional affiliations.